Spatio-temporal growth of disturbances in a boundary layer and energy based receptivity analysis

T. K. Sengupta,[a] A. Kameswara Rao, and K. Venkatasubbaiah
Department of Aerospace Engineering, Indian Institute of Technology, Kanpur 208 016, India

(Received 17 March 2006; accepted 25 July 2006; published online 11 September 2006)

In fluid dynamical systems, it is not known *a priori* whether disturbances grow either in space or in time or as spatio-temporal structures. However, for boundary layers, it is customary to treat it as a spatial problem and some limited comparison between prediction and laboratory experiments exist. In the present work, the receptivity problem of a zero pressure gradient boundary layer excited by a localized harmonic source is investigated under the general spatio-temporal framework, using the Bromwich contour integral method. While this approach has been shown to be equivalent to the spatial study, for unstable systems excited by a single frequency source [T. K. Sengupta, M. Ballav, and S. Nijhawan, Phys. Fluids **6**, 1213 (1994)], here we additionally show, how the boundary layer behaves when it is excited (i) at a single frequency that corresponds to a stable condition (given by spatial normal-mode analysis) and (ii) by wideband frequencies, that shows the possibility of flow transition due to a spatio-temporally growing forerunner or wave front. An energy based receptivity analysis tool is also developed as an alternative to traditional instability theory. Using this, we reinterpret the concept of critical layer that was originally postulated to explain the mathematical singularity of inviscid disturbance field in traditional instability theory of normal modes.
 [DOI: 10.1063/1.2348732]

I. INTRODUCTION

Hydrodynamic stability theory is considered the bridge linking laminar and turbulent flows, which is an area of significant activity.[1,2] Despite significant advances made, there are issues of flow transition that remain incompletely understood. Classical approaches to the instability studies involve identifying an equilibrium state, whose stability is studied by eigenvalue analysis by linearizing the governing equations. Eigenvalue analyses seek the least stable eigenmode of the linearized mass and momentum conservation equations suitably transformed to the Orr-Sommerfeld equation[3,4] via parallel flow approximation and whose solution is usually known as the Tollmien-Schlichting (TS) waves. It is also known that equilibrium flow profiles without any inflection point, support two-dimensional TS waves that arise due to viscous instability. The Reynolds number (Re) at which the equilibrium flow becomes unstable for the first time for any harmonic excitation, is known as the critical Reynolds number (Re_{cr}).

Results obtained by eigenvalue analysis approach match with laboratory experiments for thermal and centrifugal instabilities. But, for instabilities, dictated by shear force do not match so well, e.g., (i) Couette and pipe flows are found to be linearly stable at all Re, while the former is known to suffer transition at $\mathrm{Re}=350$ computationally[5] and the latter at $\mathrm{Re}\geqslant 1950$ experimentally,[6] with the exact value dependent upon facilities and background noise level; (ii) plane Poiseuille flow has a $\mathrm{Re}_{cr}=5772$, while in the laboratory experiment transition was shown to occur at $\mathrm{Re}=1000$.[7] According to Trefethen *et al.*,[8] the other example for which *"eigenvalue analysis fails include to a lesser degree, Blasius boundary layer flow."* One of the features of traditional eigenvalue analysis is that the disturbance field is assumed to grow either in space or in time. Huerre and Monkewitz[9] have applied the combined spatio-temporal theory to a family of mixing layers with the goal of determining a general criterion whereby a class of flows can be analyzed by either the spatial or temporal theory by inspecting the dispersion relation in the complex wave number-frequency plane.

The overemphasis of the least stable mode in eigenvalue analysis is rectified in receptivity analysis, as shown for the Blasius boundary layer[3,10–12] with the parallel flow approximation by assuming the disturbances to vary spatially for fixed frequency harmonic excitation at the wall. This is known as the *signal problem* in receptivity analysis. The essential difference between eigenvalue and receptivity analyses lies in the fact that the latter is capable of accounting for the effects of all eigenmodes. In the spatial approach, the disturbance stream function is obtained by performing the Bromwich contour integral,[13,14]

$$\psi(x,y,t)=\frac{e^{-i\beta_0 t}}{2\pi}\int_{\mathrm{Br}}\phi(y,\alpha,\beta_0)e^{i\alpha x}d\alpha, \tag{1}$$

where β_0 is the circular frequency of excitation and Br indicates the Bromwich contour followed in evaluating the above integral in the complex α plane. The bilateral Laplace transform ϕ is obtained as a solution of the Orr-Sommerfeld equation (5).

The assumption that the boundary layer responds at the same frequency of the exciter in the *signal problem* is improper, especially for absolutely unstable systems for which the transients associated with finite startup can land the sys-

[a]Electronic mail: tksen@iitk.ac.in

tem at the absolute frequency that can be far removed from β_0. In Ref. 15, spatio-temporal theory was used to ascertain the inviscid instability of jets and wakes to provide an estimate of the Strouhal number. Similarly, the receptivity problem of wave-packet propagation created by a single pulse was studied earlier in the context of a stationary phase asymptotic solution obtained by the saddle point method.[4,15] A conclusion was reached that out of all singularities, those corresponding to zero group velocity are the important ones. In contrast to these spatio-temporal approaches, a complete spatio-temporal growth of the disturbances and their evolution to Tollmien-Schlichting (TS) waves was studied in Sengupta *et al.*[16]

It is appropriate to place the present work with the 2D perturbation field, in the context of other researches that predict very large transient growth of disturbances. It has been shown[2] that the regular and adjoint solutions of Orr-Sommerfeld equations are orthogonal, however Orr-Sommerfeld eigenfunctions are not orthogonal to each other. This leads to the sensitivity of the eigenvalues to perturbations to the underlying stability operator, as shown for channel flows. It has, however, been pointed out that the *non-normality of the Orr-Sommerfeld operator not only has consequences for the sensitivity of the spectrum, but it also influences the dynamics of disturbances governed by the linearized Navier-Stokes equations.* This causes transient growth noted by various researchers (see, e.g., Schmid[17]) who have reported maximum transient growth rates for Blasius boundary layers for a flow at Re=1000 (see also Fig. 4.6 in Schmid and Henningson[2]). This figure shows that more than a 1000-fold growth is possible for general 3D disturbance fields. However, for 2D disturbance fields, corresponding maximum transient growth rates are very small. This has been clearly stated in Trefethen *et al.*[8] that the *"essential feature of this nonmodal amplification is that it applies to three-dimensional (3D) perturbation of the laminar flow field…. When only 2D perturbations are considered, some amplification can still occur, but it is far weaker."*

In view of the discussion in the previous paragraph, we note that the difference between the spatio-temporal growth of the leading wave front shown here from that shown in the transient growth studies.[2,8,17] The present focus is upon the 2D disturbance field that grows at a very high rate simultaneously in space and time, not simply in transient fashion.

There is a major difference between the asymptotic stability analysis[18] and the receptivity analysis.[11,12,19] By definition, the stability analysis provides a solution that is valid for locations, far away from the source of excitation. In contrast, the receptivity analysis provides a solution that is valid across all locations, including the upstream part of the exciter. We also note that the present receptivity study is given here for a two-dimensional disturbance field; there are many other asymptotic stability studies involving algebraic or transient growth of three-dimensional disturbance field.[20]

Instead of studying stability using mass and momentum conservation, alternate approaches based on energy consideration had been initiated[2,21] leading to the well known Reynolds-Orr equation. This equation deals with the evolution of the disturbance field in terms of its kinetic energy, that is briefly discussed in the following.

If we write the Navier-Stokes equation in the indicial notation and take a dot product of it with the velocity vector we get the following:[2]

$$u_i\frac{\partial u_i}{\partial t} = -u_iu_j\frac{\partial U_i}{\partial x_j} - \frac{1}{\mathrm{Re}}\frac{\partial u_i}{\partial x_j}\frac{\partial u_i}{\partial x_j} + \frac{\partial}{\partial x_j} \times\left[-\frac{1}{2}u_iu_iU_j - \frac{1}{2}u_iu_iu_j - u_ip\delta_{ij} + \frac{1}{\mathrm{Re}}u_i\frac{\partial u_i}{\partial x_j}\right].$$

If one defines the kinetic energy of the full domain as $E_V=1/2\int_V u_iu_i dV$ then the above can be integrated over the whole domain to give rise to the Reynolds-Orr equation as

$$\frac{dE_V}{dt} = -\int_V u_iu_j\frac{\partial U_i}{\partial x_j}dV - \frac{1}{\mathrm{Re}}\int_V \frac{\partial u_i}{\partial x_j}\frac{\partial u_i}{\partial x_j}dV.$$

This equation is derived subject to the assumption that the disturbance field is localized and spatially periodic. This assumption removes any contribution coming from the nonlinear terms. Discussion of hydrodynamic instability based on energy principles have also been described earlier.[22,23] Stuart[23] specifically points out that various estimates of critical Reynolds number obtained by this approach are erroneously low due to the assumption of disturbance field being localized and/ or spatially periodic that leads to the elimination of nonlinear disturbance terms appearing in the divergence form of the equations of motion. In the present work, we propose a new energy-based receptivity analysis, based on the Navier-Stokes equation without making any assumptions. The key difference comes in the way the energy is defined in the present exercise, as discussed below. Also, our procedure retains the nonlinear term contribution (as we do not make any assumption of spatial periodicity or localized nature of excitation), and the contribution of nonlinear terms are central to any instability studies.

In this context, Landahl and Mollo-Christensen[24] have stated that a proper understanding of flow instability requires a study of *"total mechanical energy of the flow (not just how the "energy of the perturbation" given by the square of the fluctuation velocity changes locally with time…)."* These deficiencies of the energy approaches can be rectified by predicting instability by a new method[25] based on total mechanical energy, whose main features are restated here. In this method, the total mechanical energy of an incompressible flow is taken as $E=p/\rho+V^2/2$, whose governing equation is obtained from the Navier-Stokes equation without any assumption as

$$\nabla^2 E = \nabla\cdot(V\times\omega). \tag{2}$$

This equation is further simplified using the identity $\nabla\cdot(V\times\omega)=|\omega|^2-V\cdot\nabla\times\omega$ and splitting E into a mean and a disturbance part, $E=E_m+\epsilon E_d$ with respect to a suitably small parameter ϵ, into the following equation for the disturbance energy (E_d):

$$\nabla^2 E_d = 2\omega_m\,.\,\omega_d + \omega_d\,.\,\omega_d - V_m\,.\,\nabla\times\omega_d - V_d\,.\,\nabla\times\omega_m - V_d\,.\,\nabla\times\omega_d. \tag{3}$$

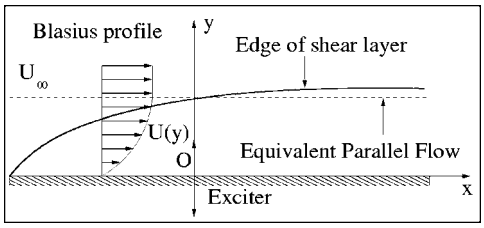

FIG. 1. Problem in the physical plane.

The subscripts *m* and *d* in these equations refer to primary and disturbance field components. This generic mechanism of instability, based on the full Navier-Stokes equation, can be used for all incompressible flows, without any need for linearization and we note that the mechanism is same for both two- and three-dimensional flows. Here, we have used this new energy based approach to explore disturbance growth and its structure inside the shear layer in the spatio-temporal framework.[16]

It is to be noted that this energy-based receptivity analysis is all-inclusive as it is based on full Navier-Stokes equation without any assumptions. Thus, all the traditional analysis methods are also defined by this equation. We will provide the connection between these two approaches in Sec. III A.

The energy based receptivity study will also allow us to reinterpret the concept of critical layer. In traditional stability theory, a critical layer *arises as a mathematical singularity for a single normal mode in an inviscid fluid*,[1] because it is well known that the Orr-Sommerfeld equation is regular at the critical layer. In the inviscid analysis, the Reynolds stress is also discontinuous across the critical layer-the discontinuity disappearing when viscous disturbance equations are considered. Furthermore, it is noted that normal modes of different wavelengths have different critical layers and hence a linear superposition of these should smooth out the singularity for arbitrary excitation of the shear layer in the linear theory. Drazin and Reid[1] have remarked that "*only the grossest properties, if any, of critical layers of homogeneous fluids have been directly observed in experiments or Nature,*" questioning the very concept of critical layers. When the mathematical singularity is removed by including weak nonlinearity in the inviscid analysis, the structure of the critical layer changes qualitatively as shown in Maslowe[26] and other references contained therein. Thus, it appears that the role and structure of critical layer is not completely clear and is also the reason for undertaking the present work.

In a recent work,[19] results have been reported on the spatio-temporal growing wave fronts for stable systems using the same methodologies employed here. It is shown that the stable systems with multiple modes display a growing wave front at the leading edge of the disturbance packet, only for parameter values for which the system possesses more than one mode.

The paper is structured in the following manner: In Sec. II, the governing equation and numerical methods used for the present study are given. In Sec. III, results of case studies are presented to highlight different aspects of receptivity, critical layer, and propagation characteristics of waves.

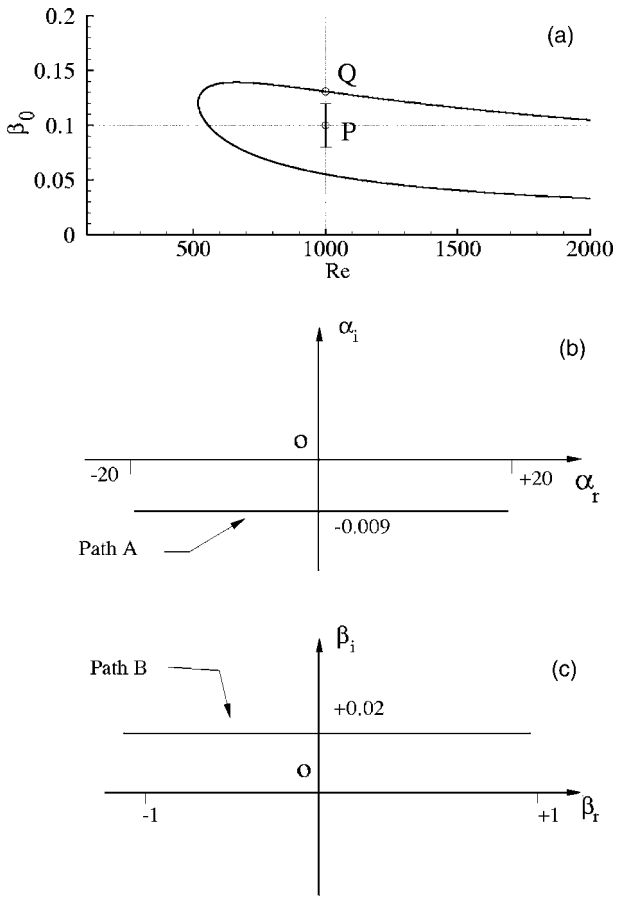

FIG. 2. (a) Neutral curve for the Blasius boundary layer. Locations of Bromwich contours in the (b) α and (c) β planes.

II. GOVERNING EQUATIONS AND NUMERICAL METHODS

The physical problem that is studied here is shown in Fig. 1, where the 2D incompressible boundary layer developing over the flat plate is excited by a localized impulsively started harmonic source located at the origin of the coordinate system. In the method to be employed, an equivalent parallel shear layer is considered that has the same thickness at the position of the exciter and is shown by the dotted line. Let the disturbance created by this excitation be given by the stream-function,

$$\psi(x,y,t) = \frac{1}{(2\pi)^2} \int \int_{\mathrm{Br}} \phi(\alpha,\beta,y) e^{i(\alpha x - \beta t)} d\alpha d\beta, \qquad (4)$$

where Br indicates the Bromwich contours followed in evaluating the above integral in the complex α and β plane. The mathematical basis of choosing Bromwich contours is to identify appropriate strips of convergence in the α and β plane,[13,14] so that the integrals in (4) do not diverge. Identifying and using appropriate Bromwich contours for the

spatio-temporal problem of viscous flow receptivity is given in Ref. 16 and a typical schematic is shown in Figs. 2(b) and 2(c).

If all lengths are nondimensionalized by δ^* (displacement thickness of the parallel shear layer), velocities by free-stream value U_∞ and time by δ^*/U_∞, then the Reynolds number is defined as $\mathrm{Re}=\delta^* U_\infty/\nu$. The bilateral Laplace transform in (4) is governed by the Orr-Sommerfeld equation given by

$$\left[\bar{U}(y)-\frac{\beta}{\alpha}\right](\phi''-\alpha^2\phi)-\bar{U}''(y)\phi = \frac{1}{i\alpha\,\mathrm{Re}}(\phi^{iv}-2\alpha^2\phi''+\alpha^4\phi), \tag{5}$$

where $\bar{U}(y)$ is the parallel mean flow and the primes indicating differentiation with respect to y. For the physical excitation shown in Fig. 1, the boundary conditions at $y=0$ are

$$u_d=0, \tag{6}$$

$$\psi(x,0,t)=H(t)\delta(x)e^{-i\beta_0 t}, \tag{7}$$

and at the far stream $(y\to\infty)$: $u_d, v_d\to 0$.

The boundary conditions to solve (5) is obtained by using (4) in the above to yield the four conditions,

$$\phi'(\alpha,\beta,y=0)=0, \tag{8}$$

$$\phi(\alpha,\beta,y=0)=\frac{1}{i(\beta_0-\beta)}, \tag{9}$$

$$\phi(\alpha,\beta,y\to\infty)\to 0, \tag{10}$$

$$\phi'(\alpha,\beta,y\to\infty)\to 0. \tag{11}$$

Effects of periodic suction and blowing at the origin at the prescribed frequency of β_0 is given by Eq. (7) or (9) and in these $\delta(x)$ is the Dirac delta function indicating the localized nature of the excitation and $H(t)$ is the Heaviside function indicating the onset of periodic excitation impulsively at $t=0$. Thus, to calculate the disturbance velocity components, one solves Eq. (5) subject to boundary conditions (8)–(11). The solution that satisfies the boundary conditions (10) and (11) and obtained here numerically is given by

$$\psi(x,y,t)=\frac{1}{(2\pi)^2}\int\int_{\mathrm{Br}}\frac{\phi_1(\alpha,\beta;y)\phi'_{30}-\phi_3(\alpha,\beta;y)\phi'_{10}}{i(\phi'_{30}\phi_{10}-\phi_{30}\phi'_{10})(\beta_0-\beta)} \times e^{i(\alpha x-\beta t)}d\alpha d\beta,$$

where ϕ_1 and ϕ_3 are the decaying inviscid and viscous modes, respectively. Additional subscript 0 refers to the variable evaluated at the wall. The first factor in the denominator of this expression is nothing but the dispersion relation of the problem and identifies the eigenvalue of the corresponding *signal problem*. Thus, this expression connects the eigenvalue and receptivity approach, where for the latter the asymptotic solutions are given by the poles of the integrand of the above relation.

One of the aims of the present work is to solve for E_d in the whole flow field. For the Blasius profile, $\mathbf{V}_m=\hat{i}U$, and Eq. (3) simplifies upon linearization as

$$\nabla^2 E_d=-2\frac{dU}{dy}\omega_d+U\nabla^2 u_d+u_d\frac{d^2U}{dy^2}. \tag{12}$$

When Eq. (4) is used to redefine the right-hand side of the above, one gets the following equation for the bilateral Laplace amplitude E_d as

$$\hat{E}_d''-\alpha^2\hat{E}_d=\phi'''U+2\phi''U'+\phi'(U''-\alpha^2U)-2\phi\alpha^2U' \tag{13}$$

when E_d is represented as

$$E_d(x,y,t)=\frac{1}{(2\pi)^2}\int\int_{\mathrm{Br}}\hat{E}_d(y)e^{i(\alpha x-\beta t)}d\alpha d\beta. \tag{14}$$

For the problem of Fig. 1, Eq. (13) needs to be solved from the free-stream to the wall, subject to the initial condition (at $y\to\infty$): $\hat{E}_d\to 0$. Equation (13) has two characteristic exponents, $\pm\alpha$ out of which the growing mode $(+\alpha)$ has to be suppressed during the solution procedure as we are interested in the wall excitation problem for which all perturbations decay as one moves far away from the wall. Solution of (13) requires one to remove any remnants of the growing mode, otherwise parasitic error will follow this and contaminate the solution. We have devised a simple filtering procedure to rectify the situation, as outlined below.

Let us say, that we have a correct solution at $y+\Delta y$ given by $\hat{E}_{do}$ and we have integrated (13) by any integration procedure to the new level at y to get the numerical solution as $\hat{E}_{dn}$. These two solutions can be written down as

$$\hat{E}_{do}\sim a_1e^{-\alpha(y+\Delta y)}+a_2e^{\alpha(y+\Delta y)}, \tag{15}$$

$$\hat{E}_{dn}\sim a_1e^{-\alpha y}+a_2e^{\alpha y}. \tag{16}$$

One can filter out the spurious growing mode contribution $a_2e^{\alpha y}$ from $\hat{E}_{dn}$ using the above numerical solutions to get the filtered solution as

$$\hat{E}_d(y)=\frac{e^{\alpha\Delta y}}{e^{2\alpha\Delta y}-1}[\hat{E}_{dn}e^{\alpha\Delta y}-\hat{E}_{do}]. \tag{17}$$

III. RECEPTIVITY OF THE BLASIUS BOUNDARY LAYER TO WALL EXCITATION

To discuss the major issues of receptivity of the wall boundary layer, we consider a case for which $\mathrm{Re}=1000$ and $\beta_0=0.1$, the same parameters used in Ref. 16 identified as point P in Fig. 2(a). Here, we have taken 8192 points from -20 to $+20$ and 512 points from -1 to $+1$ in α and β planes, respectively. These are twice as many points taken, in each plane to that were used in Ref. 16, so that the solution is obtained for longer duration and over a longer stretch in the streamwise direction. The Orr-Sommerfeld equation is solved in $0\leqslant y\leqslant 6.97$ with 2400 points as compared to 1200 points used in Ref. 16. For this parameter combination, the Blasius boundary layer has three modes—one unstable and

the other two being stable and it was seen earlier[16] that the evolving space-time dependent solution is same as that obtained from the spatial receptivity analysis.[11] Thus, the spatio-temporal treatment produced a solution that is dominated by the unstable mode, with the damped mode playing no role.

For this case, the unstable mode is at $\alpha^* = (0.279\,827, -0.007\,287\,21)$ that is a downstream propagating mode with a group velocity of 0.4202.[16] The choice of the Bromwich contour reflects this fact, as the Bromwich contour in the α plane is below and parallel to α_{real} axis at a distance of 0.009 and in the β plane it is above and parallel to the real axis at a distance of 0.02. The other two eigenvalues, are also downstream propagating with positive imaginary part for α.

The Orr-Sommerfeld equation has been solved by the compound matrix method (CMM).[1,16] It has also been shown[16] that CMM has problems at high α due to stiffness of the original problem. It is for this reason the solution is filtered further by the following:

$$G(\alpha) = \frac{q_{-2}e^{-2i\alpha} + q_{-1}e^{-i\alpha} + q_0 + q_1 e^{i\alpha} + q_2 e^{2i\alpha}}{p_{-1}e^{-i\alpha} + 1 + p_1 e^{i\alpha}}, \qquad (18)$$

where $p_{\pm 1} = D \pm \eta/60$, $q_{\pm 2} = \pm F + \eta/300$, $q_{\pm 1} = \pm E + \eta/30$, and $q_0 = -11\eta/150$ with $D = 0.379\,389\,491\,2$, $E = 0.787\,786\,8$, $F = 0.045\,801\,2$ and $\eta = -2$. These types of filters are often employed for direct numerical simulation. This only smooths the data at the extreme ends of the Bromwich contour in the α plane, as shown along path A in Fig. 2(b). In the β plane a traditional Hanning window[16] is employed for the solution along the path B in Fig. 2(c).

Computed disturbance streamwise velocity component (u_d) is shown in Fig. 3, as a function of x for the indicated time frames at $y = 0.278$, where $x = 0$ corresponds to the location of the exciter. During the evolution of disturbances, we note three distinct components in Fig. 3: (i) a local solution in the immediate neighborhood of the exciter, (ii) an asymptotic part that displays the growing unstable solution with the growth rate as given by the spatial eigenvalue analysis, and (iii) the disturbance front or the leading edge of the evolving wave-packet. If we look at the streamwise disturbance velocity data at $t = 411.5$ and look for one spatial period to calculate the wave number of the response fields, we find this as $\alpha_r = 0.277\,940$. Also by noting the peak values of u_d at two successive crests, we calculate the growth rate of the wave train as $\alpha_i = -0.007\,278$. These two values compare extremely well with the values obtained by the eigenvalue analysis for Re = 1000 and $\beta_0 = 0.1$ for the unstable mode. Thus, the present method of calculating the response of the system by the combined spatio-temporal receptivity analysis yields very satisfactory results for the asymptotic part and additionally, we obtain the wave front and the local solution, those are not available by any other means. It is also noted that for single frequency excitation, for which the spatial analysis indicates instability, both the spatial and spatio-temporal receptivity analyses produce identical results.

The above observation on the equivalence of spatial and spatio-temporal analysis for Blasius boundary layer excited by a single frequency, that leads to spatial instability raises the question whether one can also extend the equivalence for neutral or stable systems. This question arises as the presence of multiple modes of similar spatial growth or decay rate can interfere among themselves to invalidate the spatial receptivity approach. Specially the neutral stability case is of interest, as it is common to both spatial and temporal eigenvalue analysis. This is investigated here, by considering the following case for which Re = 1000 and $\beta_0 = 0.1307$, corresponding to the point Q, on the upper branch of the neutral curve, as shown in Fig. 2(a). Computed results are shown in Fig. 4 for

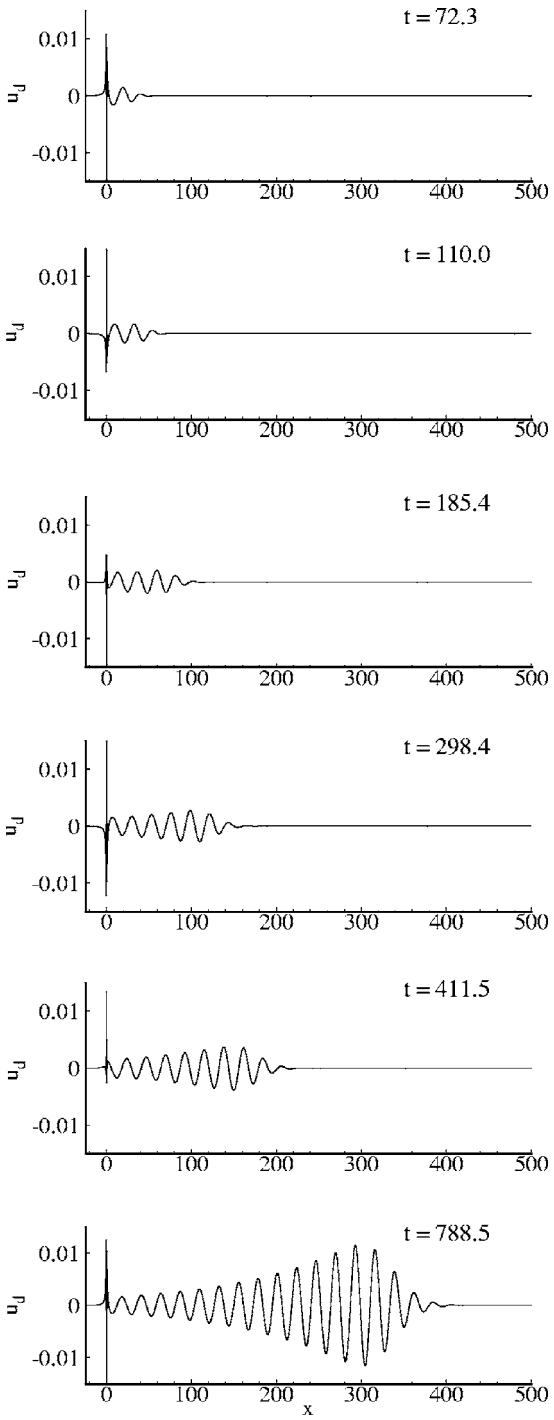

FIG. 3. Streamwise disturbance velocity plotted as a function of x at indicated times for Re = 1000, $\beta_0 = 0.1$, and $y = 0.278$.

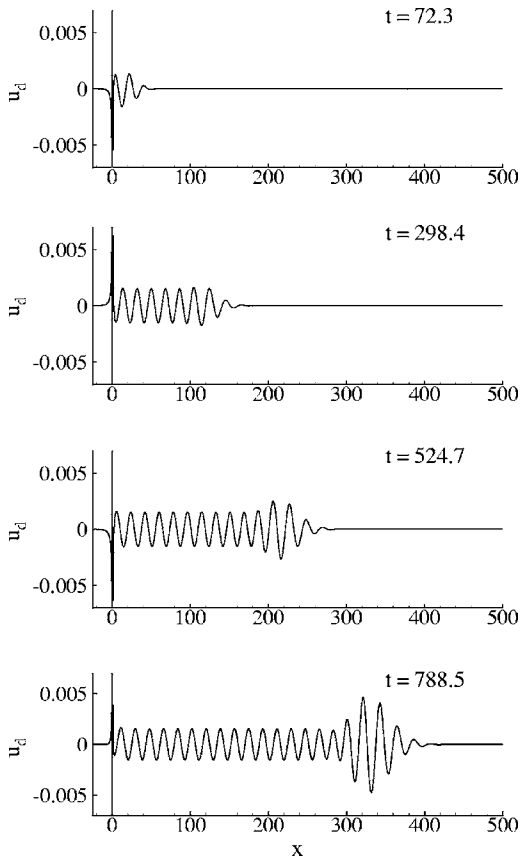

FIG. 4. Streamwise disturbance velocity plotted as a function of x at indicated times for Re=1000, β_0=0.1307, and y=0.278.

the indicated time frames that indicate neutrally stable variation of the asymptotic part of the signal. However, one notices that there is a constantly growing wave front in this case. The growth of this front is both in space and in time, that is sustained. Presence of the spatio-temporally growing wave front is to be contrasted with the transient growth attributed to *nonorthogonal* or *nonmodal* eigenvectors[27,28] to explain the subcritical transition for systems that have been pronounced stable by normal mode eigenvalue analysis. The main difference between the present analysis and the method based on nonmodal amplification theory is that the former is shown here for two-dimensional disturbance field, while the latter applies only to three-dimensional perturbation.[8] However, it is possible to extend the present method for the three-dimensional disturbances field also. Thus, in contrast to the nonmodal amplification theories[8] and/or algebraic growth asymptotic analysis method[20] being applicable to three-dimensional fields only, the present method is more general as shown here for the two-dimensional flow field.

The above cases studied with the help of spatio-temporal receptivity analysis revealed that when the Blasius boundary layer is excited by a single frequency source at the wall, the presence of a distinct wave front is indicated for systems for which the leading eigenmode is either neutrally stable (as in Fig. 4) or stable.[19] For the case of Fig. 3, the wave front is dominated by the unstable normal mode. In contrast, for the case of Re=1000 and β_0=0.1307, there are three modes present, whose location in the complex α plane are given by α_1=(0.349 823 9, 0.0), α_2=(0.214 917 7, 0.145 464 3), and α_3=(0.160 402 5, 0.259 302 8) and the total response field is due to the neutral mode, as well as the interaction between the damped modes. We reiterate that the growing wave front is only feasible for stable or neutrally stable system with multiple modes—which is due to constructive interference of the damped modes—that are essentially the orthogonal modes of the Orr-Sommerfeld equation and not the non-normal modes discussed in the literature,[8] as explained in the Introduction.

It is noted that for this case, as well as for the unstable case of Fig. 3, the wave front propagates at the speed V_g=0.483. According to Sommerfeld,[29] for the propagation of light in dispersive media, the front of the signal propagates, under all circumstances, with the phase speed. This is not the case here, as the wave front speed is significantly different from the phase speed (given, respectively, as 0.3736, 0.6081, and 0.8148) or the group velocity (given, respectively, as 0.4261, 0.3097, and 0.1231) of the three present modes. In the same way, the dominant wave number of the modulated waves inside the wave front has α_{real} =0.30, that is different from the wave number of any of the constituent modes.

To emphasize the role of mode interactions is investigated next, for basically unstable cases, when the Blasius boundary layer is excited by a wideband source at the wall as identified in Fig. 2(a) around point P. To ascertain the features of the wave front, we consider the case of wideband excitation at $\beta_0=0.1\pm0.02$. If we express the solution of the parallel boundary layer to an impulsively started harmonic excitation at β_0 as

$$\psi(x,y,t;\beta_0)=\frac{1}{(2\pi)^2}\int\int_{\text{Br}}\frac{\phi_1(\alpha,\beta;y)\phi'_{30}-\phi_3(\alpha,\beta;y)\phi'_{10}}{i(\phi'_{30}\phi_{10}-\phi_{30}\phi'_{10})(\beta_0-\beta)}\times e^{i(\alpha x-\beta t)}d\alpha d\beta, \tag{19}$$

then the solution for the banded excitation case is obtained from the convolution given by

$$\psi(x,y,t,\beta_1,\beta_2)=\int_{\beta_1}^{\beta_2}\psi(x,y,t;\beta_0)d\beta_0. \tag{20}$$

Here, β_1 and β_2 defines the bandwidth of the excitation. The chosen band here is such that for every frequency component, the fundamental mode indicates instability as shown in Fig. 3. For the banded excitation, each unstable mode will interact with each other to create further wave packets and it would be interesting to note whether all the unstable modes would reinforce or attenuate each other.

Results for the streamwise component of disturbance velocity is shown plotted in Fig. 5 at the indicated time instants. One notices that up to t=110.0, results are identical in Figs. 3 and 5, and effect of the frequency band is not perceptible. This is due to the fact that the evanescent waves in either cases are dominated by the local solution. However, from t=185.4 onwards, the presence of multiple frequencies are seen behind the leading wave front. There appears to be significant cancellations among different unstable waves at the back of the wave front starting from this time on. As a

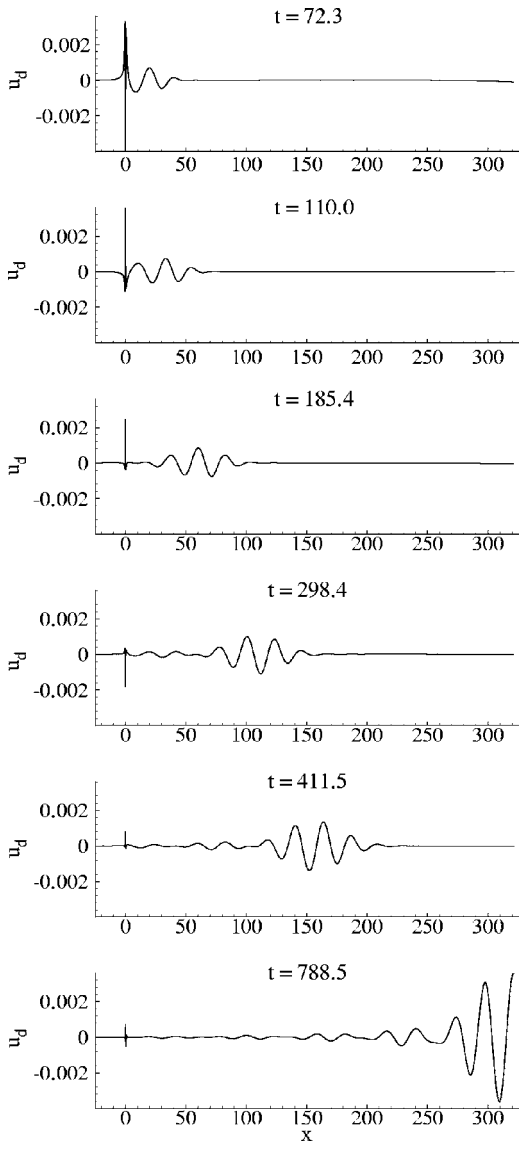

FIG. 5. Streamwise disturbance velocity plotted as a function of x at indicated times for banded excitation centered around $\beta_0=0.1$, $\Delta\beta=\pm0.02$, Re=1000, and $y=0.278$.

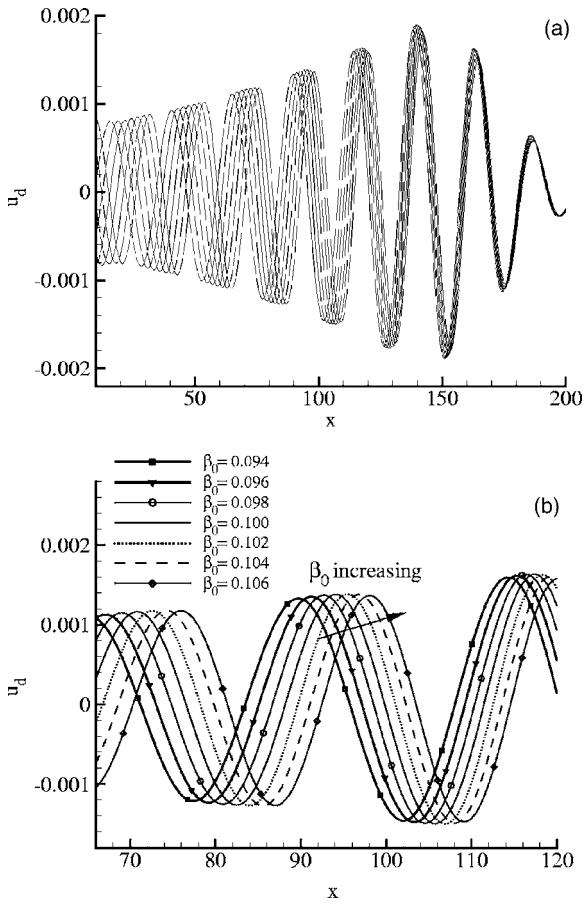

FIG. 6. (a) Streamwise disturbance velocity plotted as a function of x at $t=411.5$ for different β_0, Re=1000, $y=0.278$. (b) Enlarged view of (a).

net result, one notices attenuated multiple packets traveling downstream, except the leading wave front that continues to grow. This is a demonstration of multiple unstable waves annihilating each other (including the local solution), while leaving a growing wave front.

The feature of signal cancellation of unstable wave systems can be better understood, if we look at some representative harmonic components of the response field in an enlarged view. In Fig. 6(a), the streamwise disturbance velocity component of various circular frequencies as a function of space for $t=411.5$ are shown. Here, only seven distinct circular frequencies are shown for the purpose of explanation. Significant phase shifts among these seven solutions for $x \leqslant 120$, are responsible for mutual cancellation of the signal. The signal components show lesser phase difference at the right of the frame. The region of x where there is significant signal cancellation has been shown enlarged in Fig. 6(b).

A. An energy-based receptivity analysis

Having obtained the disturbance velocity components, we solve Eq. (13) for the disturbance energy amplitude as a function of α and β. From the solution one can reconstruct E_d as a function of x and t by performing Bromwich integrals successively in Eq. (14). In Fig. 7, variation of E_d, as a function of x at discrete times, is shown at the inner maximum ($y=0.278$) for the case of Fig. 3. Unlike the velocity field, the variation of E_d across the exciter is smoother, specifically in the upstream direction ($x \leqslant 0$). One notes the growing E_d following the leading wave front.

One can calculate the wavelength and the growth rate of E_d from Fig. 7, that provides the value of the complex wave number as $\alpha=(0.277\,974,\ -0.007\,362)$ that matches very well from the value obtained from Fig. 3, for u_d as $\alpha=(0.277\,940,\ -0.007\,278)$. These values, in turn, compare well with the value obtained by eigenvalue analysis quoted before.

Variation of E_d with y is shown in Fig. 8, at two different streamwise stations ($x=65.66$ and 129.9) for different times. In these figures, we have marked the location of the point (y_c) where $U(y_c)$ is equal to the phase speed, c of the fundamental mode, usually referred to as the critical layer. The streamwise disturbance velocity has a logarithmic singularity of the type $U''(y_c)/U'(y_c)\ln(y-y_c)$ at this height shown for inviscid analysis. To remove this singularity of inviscid nor-

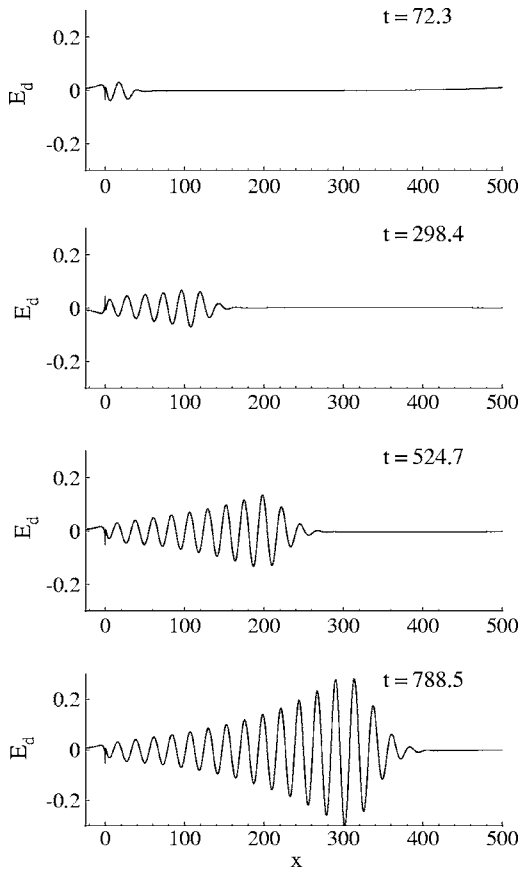

FIG. 7. Disturbance energy plotted as a function of x at indicated times for Re=1000, β_0=0.1, and y=0.278.

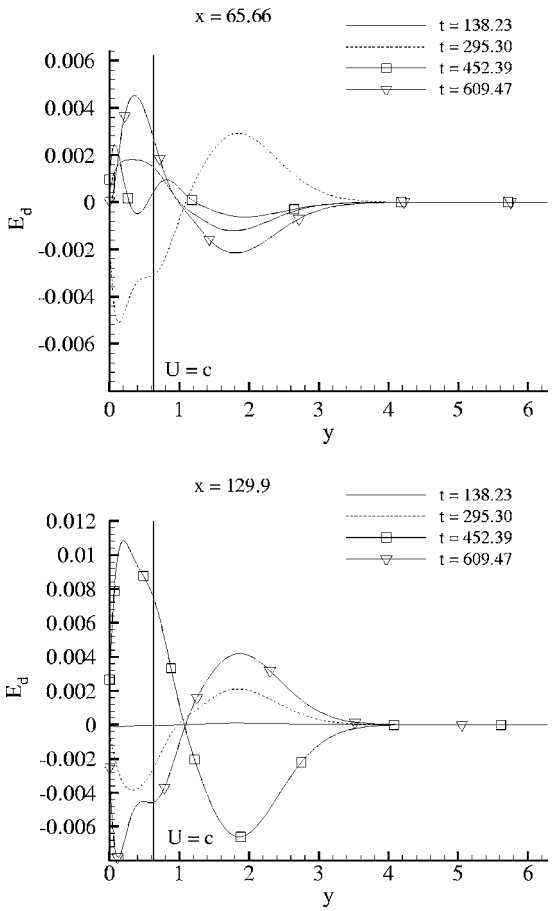

FIG. 8. Disturbance energy plotted as a function of y at indicated x and t for Re=1000, β_0=0.1.

mal mode disturbances, Lin[22] suggested restoring viscosity within a thin critical layer around y_c. Also, an expression for dimensionless Reynolds stress averaged over a wavelength displays, across this singular point, a discontinuity given by $\alpha U''(y_c)/U'(y_c)|\phi(y_c)|^2$ and it has often been suggested[26] that this discontinuity gives rise to the oscillation that are responsible for creating the Tollmien-Schlichting waves. Present spatio-temporal receptivity analyses clearly show that there are no singularities seen in the solution of Orr-Sommerfeld equation and the E_d growth is governed by Eq. (13) and maximum for E_d is not located where $U=c$. The structure of E_d also reveals a single outer maximum that is far above the outer maximum noted for the velocity field. Also, one notices multiple maxima for E_d near the wall, unlike the structure for u_d (not shown). None of the maximum of E_d near the wall are located where U is equal to c of any of the modes.

IV. SUMMARY

A spatio-temporal receptivity analysis is conducted here for the Blasius boundary layer, when it is excited at the wall by single and wideband frequency sources. It is noted that for single frequency excitation cases, if the underlying boundary layer is found to be unstable by spatial eigenvalue analysis, then the spatial and spatio-temporal receptivity analysis produce identical response field, as shown earlier[16] and re-established here in Fig. 3, by conducting calculations over a longer domain and longer time. The response field is composed of a local component, an asymptotic part of the solution and a wave front. It is shown that the unstable mode dictate the response field solely in terms of the asymptotic component and the wave front.

Difference between the spatial and spatio-temporal analysis method emerge, for neutrally stable and stable systems. This is due to interactions of modes that have similar amplitude and phase relationship for stable or neutrally stable systems, with the stable modes reinforcing each other at the wave front. It is shown here, for a neutrally stable system, in Fig. 4, where the neutrally stable mode determines the asymptotic part of the solution. The wave front indicates a constructive interference between multiple stable modes. This is also equally true for stable systems.[19]

The centrality of mode interactions is also established by considering a wideband excitation case. The frequency band of the exciter is chosen in such a way that the system is seen to be unstable by normal mode spatial eigenvalue analysis at all frequencies. However, despite the presence of individual unstable modes, mode-interaction among these creates an attenuated response field, as shown in Fig. 5. The reason for the attenuation is explained in Fig. 6, where it is shown that phase detuning at the asymptotic part of the wavetrain is responsible for this. It is also shown that such wave-cancellations are not present at the wave front, instead there is a constructive interference that causes it to grow in space

and time. All of these indicate that *a priori* one does not know where to use spatial theory and the present work points to the need for spatio-temporal approach in all receptivity analysis.

An energy based receptivity analysis is also conducted for the Blasius boundary layer, following the method[25] for bypass transition. As the receptivity equation was derived from Navier-Stokes equation without any assumption, it also applies to flow instabilities covered by linearized theories to estimate the disturbance energy (E_d) structure. The wavelength and growth rate of E_d calculated from Fig. 7 compares well with the values obtained from eigenvalue analysis. The detailed structure of E_d is shown in Figs. 7 and 8 for Re $=1000$ and $\beta_0=0.1$, that does support the existing view that the mathematical singularity disappears in the viscous flow framework and as such there is no need to invoke a critical layer.

[1] P. G. Drazin and W. Reid, *Hydrodynamic Stability* (Cambridge University Press, Cambridge, 1981).
[2] P. J. Schmid and D. S. Henningson, *Stability and Transition in Shear Flows* (Springer Verlag, New York, 2001).
[3] D. E. Ashpis and E. Reshotko, "The vibrating ribbon problem revisited," J. Fluid Mech. **213**, 531 (1990).
[4] A. Bers, in *Physique des Plasmas*, edited by C. Dewitt and J. Peyraud (Gordon and Breach, New York, 1975).
[5] A. Lundbladh and A. V. Johansson, "Direct simulation of turbulent spots in plane Couette flow," J. Fluid Mech. **229**, 499 (1991).
[6] O. Reynolds, *Scientific Papers* (Cambridge University Press, Cambridge, 1901).
[7] S. J. Davies and C. M. White, "An experimental study of the flow of water in pipes of rectangular section," Proc. R. Soc. London, Ser. A **119**, 92 (1928).
[8] L. N. Trefethen, A. E. Trefethen, S. C. Reddy, and T. A. Driscoll, "Hydrodynamic stability without eigenvalues," J. Fluid Mech. **261**, 578 (1993).
[9] P. Huerre and P. A. Monkewitz, "Absolute and convective instabilities in free shear layers," J. Fluid Mech. **159**, 151 (1985).
[10] M. Gaster, "On the generation of spatially growing waves in a boundary layer," J. Fluid Mech. **22**, 433 (1965).
[11] T. K. Sengupta, in *Proceedings of the 7th International Conference on Numerical Methods in Laminar and Turbulent Flows*, edited by C. Taylor, J. H. Chin, and G. M. Homsy (Pineridge, Swansea, 1991).
[12] M. Gaster and T. K. Sengupta, in *Instabilities and Turbulence in Engineering Flows*, edited by D. E. Ashpis, T. Gatski, and R. Hirsch (Kluwer, Dordrecht, 1993).
[13] A. Papoulis, *The Fourier Integral and Its Application* (McGraw-Hill, New York, 1962).
[14] B. Van Der Pol and H. Bremmer, *Operational Calculus Based on Two-Sided Laplace Integral* (Cambridge University Press, Cambridge, 1959).
[15] M. Gaster, "Growth of disturbances in both space and time," Phys. Fluids **11**, 723 (1968).
[16] T. K. Sengupta, M. Ballav, and S. Nijhawan, "Generation of Tollmien-Schlichting waves by harmonic excitation," Phys. Fluids **6**, 1213 (1994).
[17] P. J. Schmid, "Linear stability theory and bypass transition in shear flows," Phys. Plasmas **7**, 1788 (2000).
[18] F. Gianetti and P. Luchini, "Leading edge receptivity by adjoint methods," J. Fluid Mech. **547**, 21 (2006).
[19] T. K. Sengupta, A. Kameswara Rao, and K. Venkatasubbaiah, "Spatio-temporal growing wave-fronts in a spatially stable boundary layers," Phys. Rev. Lett. **96**, 224504 (2006).
[20] S. Zuccher, A. Bottaro, and P. Luchini, "Algebraic growth in a Blasius boundary layer," Eur. J. Mech. B/Fluids **25**, 1 (2006).
[21] W. M. F. Orr, "The stability or instability of the steady motions of a perfect liquid and of a viscous liquid. Part I: A perfect liquid. Part II: A viscous liquid," Proc. R. Ir. Acad., Sect. A **27**, 9 (1907).
[22] C. C. Lin, *The Theory of Hydrodynamic Stability* (Cambridge University Press, Cambridge, 1955).
[23] J. T. Stuart, in *Laminar Boundary Layer*, edited by L. Rosenhead (Clarendon, Oxford, 1963), p. 492.
[24] M. T. Landahl and E. Mollo-Christensen, *Turbulence and Random Processes in Fluid Mechanics* (Cambridge University Press, Cambridge, 1992).
[25] T. K. Sengupta, S. De, and S. Sarkar, "Vortex-induced instability of an incompressible wall-bounded shear layer," J. Fluid Mech. **493**, 277 (2003).
[26] S. Maslowe, "Critical layers in shear flows," Annu. Rev. Fluid Mech. **18**, 405 (1986).
[27] K. M. Butler and B. F. Farrell, "Three dimensional optimal perturbations in viscous shear flow," Phys. Fluids A **4**, 1637 (1992).
[28] S. C. Reddy and D. S. Henningson, "Energy growth in viscous channel flows," J. Fluid Mech. **252**, 209 (1993).
[29] L. Brillouin, *Wave Propagation and Group Velocity* (Academic, New York, 1960).